

Can surface flux transport account for the weak polar field in cycle 23?

Jie Jiang · Robert H. Cameron · Dieter Schmitt · Manfred Schüssler

Received: date / Accepted: date

Abstract To reproduce the weak magnetic field on the polar caps of the Sun observed during the declining phase of cycle 23 poses a challenge to surface flux transport models since this cycle has not been particularly weak. We use a well-calibrated model to evaluate the parameter changes required to obtain simulated polar fields and open flux that are consistent with the observations. We find that the low polar field of cycle 23 could be reproduced by an increase of the meridional flow by 55% in the last cycle. Alternatively, a decrease of the mean tilt angle of sunspot groups by 28% would also lead to a similarly low polar field, but cause a delay of the polar field reversals by 1.5 years in comparison to the observations.

Keywords Sun: activity · Sun: magnetic fields · Sun: photosphere

1 Introduction

The current solar minimum shows some peculiar features. There were 265 and 261 spotless days in the years 2008 and 2009, respectively. Only the years 1878, 1901 and 1913 showed more spotless days in the daily records since 1849¹. The polar field is about 40% weaker than during the previous three minima for which routine magnetograph measurements are available². Polar coronal-hole areas shrank by about 20% (Wang et al. 2009) and the heliospheric open flux reached the lowest values since systematic measurements started in 1967 (Wang et al. 2009). Observations from Ulysses showed that the high-latitude solar wind is 17% less dense and cooler than during the previous

Jie Jiang

Key Laboratory of Solar Activity, National Astronomical Observatories, Chinese Academy of Sciences, Beijing 100012, China

Max-Planck-Institut für Sonnensystemforschung, 37191 Katlenburg-Lindau, Germany

E-mail: jiejiang@nao.cas.cn

Robert H. Cameron · Dieter Schmitt · Manfred Schüssler

Max-Planck-Institut für Sonnensystemforschung, 37191 Katlenburg-Lindau, Germany

E-mail: cameron@mps.mpg.de; schmitt@mps.mpg.de; schuessler@mps.mpg.de

¹ <http://users.telenet.be/j.janssens/Spotless/Spotless.html#Year>

² <http://wso.stanford.edu/Polar.html>

solar minimum (McComas et al. 2008). The unusual properties of the polar corona, the open flux, and the solar wind are probably all closely related with the weakness of polar field.

This situation poses an interesting challenge to surface flux transport models (SFTM), which consider the passive transport and evolution of the radial component of the magnetic field on the solar surface under the effect of differential rotation, meridional flow and diffusion (Wang et al. 1989; van Ballegoijen et al. 1998; Schrijver 2001; Mackay et al. 2002; Baumann et al. 2004, 2006). Such models have been shown to be consistent with the observed evolution of the magnetic field distribution at the surface, including the reversals of the polar fields. The models take their input from the observed flux emergence (e.g., in terms of sunspot data or magnetograms), so that their results are closely tied to the activity level of the solar cycles. Since cycle 23 was not particularly weak in comparison to its predecessors, the polar fields generated by the flux transport models tend to be much stronger than observed. In this paper, we consider which changes of the parameters or input data would be required for cycle 23 in order to bring the models into agreement with the actual data.

2 Solar surface flux transport model

In a preceding study (Cameron et al. 2010), we have carried out flux transport simulations including the observed cycle-to-cycle variation of sunspot group tilt angles to model the solar surface field and open flux from 1913 to 1986, based upon the RGO and SOON sunspot area data sets³. We obtained a reasonable agreement of the time evolution of the open flux and of the reversal times of the polar fields with empirical results. Unfortunately, this model cannot easily be extended to cover the last cycles because systematic observations of tilt angles are not available and the definition of sunspot groups is inconsistent between the RGO and SOON data sets. We have therefore used the monthly international sunspot number since 1976 as the basic input quantity describing the emergence of new flux (cf. Fig. 1). This method has been validated by comparison with Cameron et al. (2010) from 1913 to 1986 (for details, see Jiang et al. 2011b).

We take the number of new bipolar magnetic regions (sunspot groups) during a given month to be proportional to the corresponding sunspot number. The SFTM then requires the prescription of latitude, longitude, area, and tilt angle for each new bipolar magnetic region. This is done on the basis of empirical relations with cycle strength together with using random numbers (for details, see Jiang et al. 2011a). As an example, Figure 2 shows the time-latitude distribution of emerging bipolar regions as model input for the three cycles considered here in comparison with the actually observed butterfly diagram.

The area of bipolar regions is chosen randomly according to the observed size distribution function (Jiang et al. 2011a), with a higher probability for large groups during cycle maximum phases (Hathaway 2010). Since preferred longitudes of flux emergence (activity nests) strongly affect the equatorial dipole component and thus the open flux during solar maxima, we draw the emergence longitudes from a combination of random longitudes with a set of longitudes clustering on two values 180 degrees apart (for details, see Jiang et al. 2011a, 2011b). On the basis of Mount Wilson and

³ <http://solarscience.msfc.nasa.gov/greenwch.shtml>

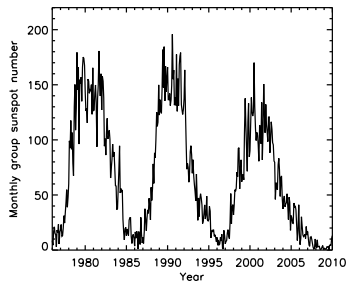


Fig. 1 Monthly international sunspot number since 1976.

Kodaikanal sunspot data, Dasi-Espuig et al. (2010) found that the average tilt angle of sunspot groups is negatively correlated with the strength of the cycle. The cycle-dependent factor T_n in the fit relation $\alpha_n(\lambda) = T_n \sqrt{\lambda}$ (α_n : average tilt angle for cycle n ; λ : latitude) is determined by using this anti-correlation (Cameron et al. 2010). The values of T_n for $n = 21, 22$, and 23 are 1.21, 1.21, and 1.32 (Jiang et al. 2011b).

The profile for the differential rotation used in our SFTM simulations is $\Omega(\lambda) = 13.38 - 2.30 \sin^2 \lambda - 1.62 \sin^4 \lambda$ (in degrees per day; Snodgrass 1983). The profile for the meridional flow is (cf. van Ballegoijen et al. 1998)

$$v(\lambda) = \begin{cases} 11 \sin(2.4\lambda) \text{ ms}^{-1} & \text{where } |\lambda| \leq 75^\circ \\ 0 & \text{otherwise,} \end{cases} \quad (1)$$

which is shown by the solid line in Figure 3. The supergranular turbulent diffusivity is chosen as $250 \text{ km}^2 \text{ s}^{-1}$ (following Schrijver and Zwaan 2000, Table 6.2).

The initial magnetic field distribution at the start of the simulation is given by Eq. 10 of Cameron et al. (2010) (see also van Ballegoijen et al. 1998). The amplitude of the initial field has been set such that the line-of-sight field averaged over a 35° wide polar cap agrees with the corresponding WSO data for 1976 (see Fig. 5). A decay term due to radial diffusion of the magnetic field (Baumann et al. 2006) has not been considered here since the observed anti-correlation of sunspot group tilt angle and cycle strength (Dasi-Espuig et al. 2010) removes the necessity for this term in short-term studies (Cameron et al. 2010). These choices of the model parameters and the flux input constitute our ‘reference model’.

3 Results of the reference model

Figure 4 shows the time evolution of the simulated radial component of the polar fields, averaged over 15° -wide polar caps. Since the location, size and emergence time of the bipolar magnetic regions involve random numbers, the results from different sets of random numbers vary somewhat. The error bars in Figure 4 denote the standard deviation for 20 runs with different random numbers. In order to compare with the line-of-sight polar field above 55° latitude observed at Wilcox Solar Observatory (WSO), we use the same definition of the polar field as WSO. The result is shown in Figure 5. The WSO polar field is multiplied by a constant factor 1.3 to correct for magnetograph saturation (Svalgaard et al. 1978). There is good agreement between the simulation and

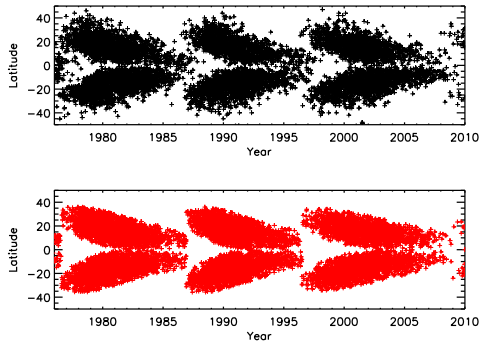


Fig. 2 Time-latitude distribution (butterfly diagram) of the bipolar magnetic regions used as input for the SFTM (lower panel) in comparison to the actual sunspot butterfly diagram from the SOON data (upper panel).

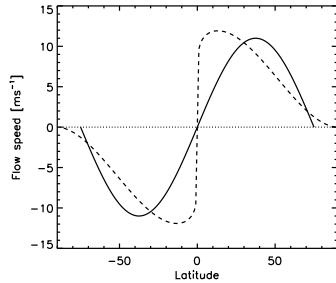


Fig. 3 Profile of meridional flow adopted in our reference model (solid curve) and the profile used by Wang et al. (2009, dashed curve).

the measurement for both the amplitude and reversal times of the polar field between 1976 and 2002. However, during the end of cycle 23, the simulation gives polar fields that are too strong by a factor of about 2.

In addition to the polar field, we also use the heliospheric open flux to compare observation and SFTM simulation. To this end, we extrapolate the simulated photospheric field out to the source surface using the current sheet source surface (CSSS) model (Zhao and Hoeksema 1995b,1995a; Jiang et al. 2010) with the model parameters given by Cameron et al. (2010). Figure 6 shows the comparison between the simulation results and the OMNI spacecraft data (with a kinematic correction, cf. Lockwood et al. 2009a).

The simulated open flux is consistent with the measurements in both maximum and minimum phases before 2005. During the minimum of cycle 23, however, the simulated result is much higher than the measurement. This is directly related to the too strong polar field since the open flux during activity minima is dominated by the low-order axial multipoles.

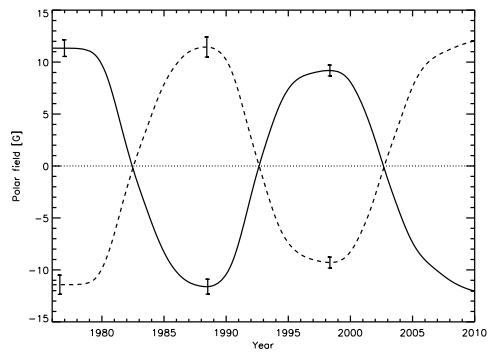


Fig. 4 Simulated evolution of radial component of solar north (full line) and south (dashed line) polar field, averaged over the 15° -wide polar caps. The error bars denote the standard deviation for 20 runs with different sets of random numbers.

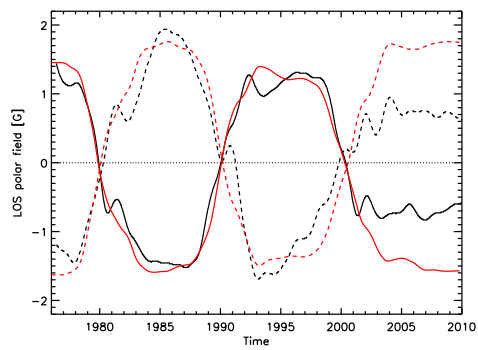


Fig. 5 Comparison between the simulated (red curves) and observed (WSO data, multiplied by a factor 1.3, black curves) line-of-sight component of solar polar field, averaged over 35° -wide polar caps. Full lines correspond to the north pole, dashed lines to the south pole.

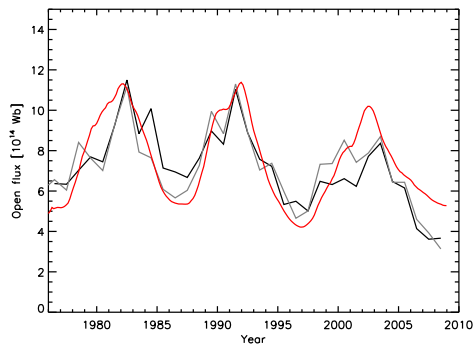


Fig. 6 Evolution of heliospheric open flux since 1976. Shown is the result of the reference SFTM (red curve) in comparison to the OMNI spacecraft data (with kinematic correction, Lockwood et al. 2009a, black curve) and values derived from geomagnetic variations (with kinematic correction, Lockwood et al. 2009b, grey curve).

4 Possible cause of the weak polar field in cycle 23

What could have been different in cycle 23? Which changes in the SFTM parameters and/or input properties could possibly lead to the low polar field? The turbulent diffusivity models the random walk of magnetic elements due to supergranular motions. Since these motions are observed to only weakly vary over the solar cycle (for a review see Rieutord and Rincon 2010, section 4.6.5), we have assumed that the diffusivity is constant in time. Likewise, the time-latitude distribution of emerging flux during cycle 23 is very similar to that of the preceding cycles (cf. Fig. 2). The same is true for the mean sunspot group areas as derived from the SOON data .

We consider three possibilities for potential parameter variations. a) sunspot number: Wilson and Hathaway (2005) found that the international sunspot number has been systematically overestimated since 1981. Lower values of the sunspot number would entail less flux emergence in our model and thus a lower polar field. b) tilt angle: although Schrijver and Liu (2008) found no indication for a systematic change in the mean tilt angle by analyzing selected MDI magnetograms, one has to keep in mind that the determined tilt angles are sensitive to the location and evolution phase (Yang et al. 2009) of the sunspot group considered, to the observer's definition, and to the instrument. Furthermore, the tilt angles show a very large scatter, possibly due to the convective buffeting of rising flux tubes in the upper layers of the convection zone (Longcope and Choudhuri 2002). c) meridional flow: significant variability of the meridional flow has been detected during cycle 23 (Chou and Dai 2001; Gizon 2004; Hathaway and Rightmire 2010; González Hernández et al. 2010). We considered variations of the meridional flow, of the mean sunspot group tilt angle, and of sunspot number during cycle 23 as potential causes of the low polar field during that cycle and used our SFTM to determine which changes of these properties in cycle 23 would be required to reproduce the observations.

Figures 7 and 8 show the evolution of the polar field and the heliospheric open flux, respectively, that result from such changes (varying one parameter at a time): a) a 40% reduction of the sunspot number (green curves), b) a 28% decrease of mean tilt angle (blue curves), or c) a 55% increase of the meridional flow (red curves), always with respect to the values for cycle 23 in the reference model. In case a), the open flux during the maximum phase of cycle 23 is much weaker than the observed value since the decreased amount of flux emergence leads to a strongly reduced equatorial dipole moment during the maximum phase. This excludes an overestimate of the sunspot number as sole cause of the low polar field. For case b), the reduced tilt angles lead to a delay of the polar field reversal by about 1.5 yrs, which is in disagreement with the observations. Smaller tilt angles correspond to less meridional magnetic flux of the bipolar magnetic regions, so that it takes longer (more bipolar regions) to reverse the polar field of the preceding cycle.

For the case c) with increased meridional flow, both polar field reversal time and amplitude match the observation (cf. Figure 7). A stronger meridional flow, especially an increased velocity gradient near the equator, effectively separates the two hemispheres, so that the transport of net flux to the poles is reduced. Although the contribution of each magnetic region to the polar field is smaller, the transport velocity is higher, thus minimizing the effect on the polar field reversal time. The increased meridional flow also brings the simulated heliospheric open flux into reasonable agreement with the observation during both the maximum and the minimum phases of cycle 23 (cf. Figure 8). This result is consistent with the SFTM simulations of Wang et al. (2009)

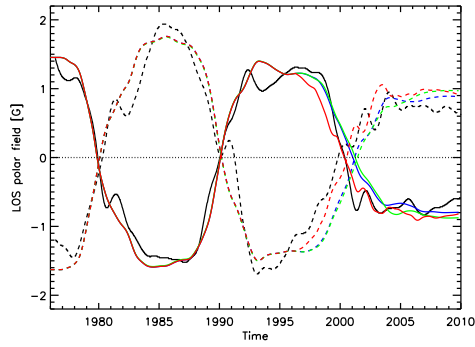


Fig. 7 Evolution of line-of-sight polar field with modified parameters during cycle 23: 40% decrease of sunspot number (green curves), 28% decrease of the sunspot group tilt angle (blue curves, which nearly lie upon the green curves), 55% increase of meridional flow (red curves). The three simulated cases are identical before the start of cycle 23. The WSO observations are given by the black curves. In all cases, full lines correspond to the north pole, dashed lines to the south pole.

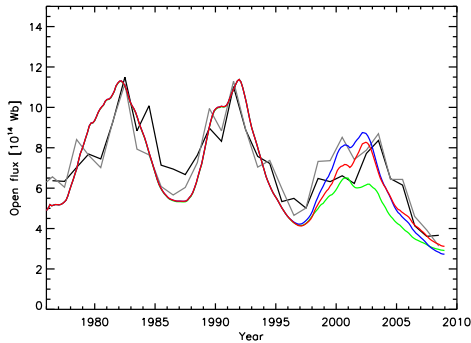


Fig. 8 Evolution of the heliospheric open flux with modified parameters during cycle 23. The colored lines refer to the same cases as in Figure 7. The black and grey lines give the OMNI data and values derived from geomagnetic variations, respectively.

and Schrijver and Liu (2008). Wang et al. (2009) found that in their model already a 15% increase of the meridional flow, much smaller than our value of 55%, is sufficient to reproduce the observed weak polar field. This is probably due to the extremely steep velocity gradient near the equator in the meridional flow profile adopted by these authors (cf. Figure 3). However, such a profile does not seem to be very realistic in the light of helioseismic measurements (e.g., Gizon and Birch 2005).

5 Conclusion

Our simulations indicate that quite substantial changes in the SFTM parameters are required to obtain the observed weak polar field during cycle 23, at least if the effect is ascribed to a change in only one parameter, such as a 28% decrease of the mean sunspot group tilt angle or a 55% increase of the meridional flow (from 11 ms^{-1} to 17 ms^{-1}).

Note that a combination of changes in more than one parameter would of course require smaller variations to bring the SFTM simulations into agreement with the observations. For instance, the results of Hathaway (2010) indicate that the meridional flow speed during the decay phase of cycle 23 was nearly 20% higher than during the corresponding phase in cycle 22. Furthermore, the meridional flow profile used in the flux transport simulation probably underestimates the poleward velocities beyond 60° latitude (Hathaway and Rightmire 2011). On the other hand, polar counterflows of the meridional flow could redistribute flux from the polar cap to lower latitudes and thus also contribute to weaker polar fields (Jiang et al. 2009). When additional empirical data (e.g., concerning the tilt angles) become available, it will be possible to further constrain the simulation parameters and hopefully achieve a better understanding of this rather unusual solar minimum.

Acknowledgements JJ thanks the organizers of Cosmic Rays in the Heliosphere II for an invitation to participate and the financial support. The National Basic Research Program of China through grants no. 10703007 and 10733020 are acknowledged for the partial funding of JJ's research.

References

- I. Baumann, D. Schmitt, M. Schüssler, A necessary extension of the surface flux transport model. *Astron. Astrophys.* **446**, 307–314 (2006). doi:10.1051/0004-6361:20053488
- I. Baumann, D. Schmitt, M. Schüssler, S.K. Solanki, Evolution of the large-scale magnetic field on the solar surface: A parameter study. *Astron. Astrophys.* **426**, 1075–1091 (2004). doi:10.1051/0004-6361:20048024
- R.H. Cameron, J. Jiang, D. Schmitt, M. Schüssler, Surface Flux Transport Modeling for Solar Cycles 15-21: Effects of Cycle-Dependent Tilt Angles of Sunspot Groups. *Astrophys. J.* **719**, 264–270 (2010). doi:10.1088/0004-637X/719/1/264
- D. Chou, D. Dai, Solar Cycle Variations of Subsurface Meridional Flows in the Sun. *Astrophys. J.* **559**, 175–178 (2001). doi:10.1086/323724
- M. Dasi-Espuig, S.K. Solanki, N.A. Krivova, R. Cameron, T. Peñuela, Sunspot group tilt angles and the strength of the solar cycle. *Astron. Astrophys.* **518**, 7 (2010). doi:10.1051/0004-6361/201014301
- L. Gizon, Helioseismology of Time-Varying Flows Through The Solar Cycle. *Solar Phys.* **224**, 217–228 (2004). doi:10.1007/s11207-005-4983-9
- L. Gizon, A.C. Birch, Local Helioseismology. *Living Reviews in Solar Physics* **2**, 6 (2005)
- I. González Hernández, R. Howe, R. Komm, F. Hill, Meridional Circulation During the Extended Solar Minimum: Another Component of the Torsional Oscillation? *Astrophys. J.* **713**, 16–20 (2010). doi:10.1088/2041-8205/713/1/L16
- D.H. Hathaway, The Solar Cycle. *Living Reviews in Solar Physics* **7**, 1 (2010)
- D.H. Hathaway, L. Rightmire, Variations in the Sun's Meridional Flow over a Solar Cycle. *Science* **327**, 1350 (2010). doi:10.1126/science.1181990
- D.H. Hathaway, L. Rightmire, Variations in the Axisymmetric Transport of Magnetic Elements on the Sun: 1996-2010. *Astrophys. J.* **729**, 80 (2011). doi:10.1088/0004-637X/729/2/80
- J. Jiang, R. Cameron, D. Schmitt, M. Schüssler, Counterflow Meridional Flow and Latitudinal Distribution of the Solar Polar Magnetic Field. *Astrophys. J.* **693**, 96–99 (2009). doi:10.1088/0004-637X/693/2/L96
- J. Jiang, R. Cameron, D. Schmitt, M. Schüssler, Modeling the Sun's Open Magnetic Flux and the Heliospheric Current Sheet. *Astrophys. J.* **709**, 301–307 (2010). doi:10.1088/0004-637X/709/1/301
- J. Jiang, R.H. Cameron, D. Schmitt, M. Schüssler, The solar magnetic field since 1700. I. Characteristics of sunspot group emergence and reconstruction of the butterfly diagram. *Astron. Astrophys.* **528**, 82 (2011a). doi:10.1051/0004-6361/201016167

-
- J. Jiang, R.H. Cameron, D. Schmitt, M. Schüssler, The solar magnetic field since 1700. II. Physical reconstruction of total, polar and open flux. *Astron. Astrophys.* **528**, 83 (2011b). doi:10.1051/0004-6361/201016168
- M. Lockwood, M. Owens, A.P. Rouillard, Excess open solar magnetic flux from satellite data: 2. A survey of kinematic effects. *J. Geophys. Res.* **114**, 11104 (2009a). doi:10.1029/2009JA014450
- M. Lockwood, A.P. Rouillard, I.D. Finch, The Rise and Fall of Open Solar Flux During the Current Grand Solar Maximum. *Astrophys. J.* **700**, 937–944 (2009b). doi:10.1088/0004-637X/700/2/937
- D. Longcope, A.R. Choudhuri, The Orientational Relaxation of Bipolar Active Regions. *Solar Phys.* **205**, 63–92 (2002)
- D.H. Mackay, E.R. Priest, M. Lockwood, The Evolution of the Sun's Open Magnetic Flux - II. Full Solar Cycle Simulations. *Solar Phys.* **209**, 287–309 (2002)
- D.J. McComas, R.W. Ebert, H.A. Elliott, B.E. Goldstein, J.T. Gosling, N.A. Schwadron, R.M. Skoug, Weaker solar wind from the polar coronal holes and the whole Sun. *Geophys. Res. Lett.* **35**, 18103 (2008). doi:10.1029/2008GL034896
- M. Rieutord, F. Rincon, The Sun's Supergranulation. *Living Reviews in Solar Physics* **7**, 2 (2010)
- C.J. Schrijver, Simulations of the Photospheric Magnetic Activity and Outer Atmospheric Radiative Losses of Cool Stars Based on Characteristics of the Solar Magnetic Field. *Astrophys. J.* **547**, 475–490 (2001)
- C.J. Schrijver, Y. Liu, The Global Solar Magnetic Field Through a Full Sunspot Cycle: Observations and Model Results. *Solar Phys.* **252**, 19–31 (2008). doi:10.1007/s11207-008-9240-6
- C.J. Schrijver, C. Zwaan, *Solar and Stellar Magnetic Activity 2000*
- M. Schüssler, I. Baumann, Modeling the Sun's open magnetic flux. *Astron. Astrophys.* **459**, 945–953 (2006). doi:10.1051/0004-6361:20065871
- N.R. Sheeley Jr., What's So Peculiar about the Cycle 23/24 Solar Minimum?, in *Astronomical Society of the Pacific Conference Series*, vol. 428, ed. by S. R. Cranmer, J. T. Hoeksema, & J. L. Kohl, 2010, p. 3
- H.B. Snodgrass, Magnetic rotation of the solar photosphere. *Astrophys. J.* **270**, 288–299 (1983). doi:10.1086/161121
- L. Svalgaard, T.L. Duvall Jr., P.H. Scherrer, The strength of the sun's polar fields. *Solar Phys.* **58**, 225–239 (1978). doi:10.1007/BF00157268
- A.A. van Ballegoijen, N.P. Cartledge, E.R. Priest, Magnetic Flux Transport and the Formation of Filament Channels on the Sun. *Astrophys. J.* **501**, 866 (1998). doi:10.1086/305823
- Y.M. Wang, A.G. Nash, N.R. Sheeley, Magnetic flux transport on the sun. *Science* **245**, 712–718 (1989)
- Y. Wang, E. Robbrecht, N.R. Sheeley, On the Weakening of the Polar Magnetic Fields during Solar Cycle 23. *Astrophys. J.* **707**, 1372–1386 (2009). doi:10.1088/0004-637X/707/2/1372
- R.M. Wilson, D.H. Hathaway, A Comparison of Rome Observatory Sunspot Area and Sunspot Number Determinations With International Measures, 1958-1998. NASA STI/Recon Technical Report N **6**, 22159 (2005)
- S. Yang, H. Zhang, J. Büchner, Magnetic helicity accumulation and tilt angle evolution of newly emerging active regions. *Astron. Astrophys.* **502**, 333–340 (2009). doi:10.1051/0004-6361/200810032
- X. Zhao, J.T. Hoeksema, Predicting the heliospheric magnetic field using the current sheet-source surface model. *Advances in Space Research* **16**, 181 (1995a). doi:10.1016/0273-1177(95)00331-8
- X. Zhao, J.T. Hoeksema, Prediction of the interplanetary magnetic field strength. *J. Geophys. Res.* **100**, 19–33 (1995b). doi:10.1029/94JA02266